Progress in Oceanography 140 (2016) 14–26

Contents lists available at ScienceDirect

Progress in Oceanography

journal homepage: www.elsevier.com/locate/pocean

Sea surface carbon dioxide at the Georgia time series site (2006–2007): Air–sea flux and controlling processes

Liang Xue [a,b], Wei-Jun Cai [b,*], Xinping Hu [c], Christopher Sabine [d], Stacy Jones [d], Adrienne J. Sutton [d,e], Li-Qing Jiang [f], Janet J. Reimer [b]

[a] Center for Ocean and Climate Research, First Institute of Oceanography, State Oceanic Administration, Qingdao 266061, China
[b] School of Marine Science and Policy, University of Delaware, Newark, DE 19716, USA
[c] Department of Physical and Environmental Sciences, Texas A&M University – Corpus Christi, Corpus Christi, TX 78412, USA
[d] Pacific Marine Environmental Laboratory, NOAA, Seattle, WA 98115, USA
[e] Joint Institute for the Study of the Atmosphere and Ocean, University of Washington, Seattle, WA 98115, USA
[f] Cooperative Institute for Climate and Satellites–Maryland, Earth System Science Interdisciplinary Center, University of Maryland, College Park, MD 20740, USA

ARTICLE INFO

Article history:
Received 15 January 2015
Received in revised form 16 September 2015
Accepted 27 September 2015
Available online 19 October 2015

ABSTRACT

Carbon dioxide partial pressure (pCO_2) in surface seawater was continuously recorded every three hours from 18 July 2006 through 31 October 2007 using a moored autonomous pCO_2 ($MAPCO_2$) system deployed on the Gray's Reef buoy off the coast of Georgia, USA. Surface water pCO_2 (average 373 ± 52 μatm) showed a clear seasonal pattern, undersaturated with respect to the atmosphere in cold months and generally oversaturated in warm months. High temporal resolution observations revealed important events not captured in previous ship-based observations, such as sporadically occurring biological CO_2 uptake during April–June 2007. In addition to a qualitative analysis of the primary drivers of pCO_2 variability based on property regressions, we quantified contributions of temperature, air–sea exchange, mixing, and biological processes to monthly pCO_2 variations using a 1-D mass budget model. Although temperature played a dominant role in the annual cycle of pCO_2, river inputs especially in the wet season, biological respiration in peak summer, and biological production during April–June 2007 also substantially influenced seawater pCO_2. Furthermore, sea surface pCO_2 was higher in September–October 2007 than in September–October 2006, associated with increased river inputs in fall 2007. On an annual basis this site was a moderate atmospheric CO_2 sink, and was autotrophic as revealed by monthly mean net community production (NCP) in the mixed layer. If the sporadic short productive events during April–May 2007 were missed by the sampling schedule, one would conclude erroneously that the site is heterotrophic. While previous ship-based pCO_2 data collected around this buoy site agreed with the buoy CO_2 data on seasonal scales, high resolution buoy observations revealed that the cruise-based surveys undersampled temporal variability in coastal waters, which could greatly bias the estimates of air–sea CO_2 fluxes or annual NCP, and even produce contradictory results.

1. Introduction

Determining mechanisms that control variations of sea surface partial pressure of carbon dioxide (pCO_2) and estimating the strength of oceanic CO_2 sink are vital for predicting future atmospheric CO_2 levels and global climate change (Benway and Doney, 2014). Given the dynamic nature of the oceanic environment particularly in terms of temporal variability, increasing research efforts have been focused on time series measurement of carbonate parameters in various parts of the global ocean (Bates et al., 2014). Time series studies have been playing an increasingly important role in understanding the ocean carbon biogeochemical cycle and the biological pump by providing concepts and observations that can be used in predictive models (Ducklow et al., 2009; Sutton et al., 2014a).

Time series observational efforts start much later and on smaller scales in coastal oceans than open ocean basins (e.g. Bates et al., 2014; Vandemark et al., 2011). Although the coastal ocean plays a disproportionately important role in the uptake of atmospheric CO_2 (0.2–0.5 Pg C yr^{-1}, 1 Pg = 10^{15} g) (Bauer et al., 2013; Borges et al., 2005; Cai, 2011; Chen et al., 2013; Fennel and Wilkin, 2009; Gattuso et al., 1998; Gruber, 2014; Laruelle et al., 2014; Muller-Karger et al., 2005), there are large uncertainties associated with estimates of air–sea CO_2 fluxes, consequently preventing accurate estimates of the global carbon budget and meaningful

* Corresponding author. Tel.: +1 302 831 2839.
E-mail address: wcai@udel.edu (W.-J. Cai).

http://dx.doi.org/10.1016/j.pocean.2015.09.008
0079-6611/

predictions of the effect of climate change on future fluxes (Bauer et al., 2013). The uncertainty is due primarily to poor spatio-temporal resolutions of field measurements, especially poor temporal coverage (e.g. Gruber, 2014) and partly to an insufficient understanding of the mechanism controlling CO_2 that also impedes modeling studies. Coastal CO_2 systems, particularly those directly influenced by riverine inputs of terrestrial carbon and nutrients, exhibit highly temporal and spatial heterogeneity (e.g. Gypens et al., 2011; Vandemark et al., 2011). Therefore, it is vital to continue and expand long-term high-resolution monitoring efforts in coastal oceans for better understanding the underlying mechanisms that control the coastal CO_2 system and how the system (e.g. status of CO_2 sink) is affected by terrestrial inputs and climate change (e.g. Bauer et al., 2013; Cai, 2011; Gruber, 2014).

It is also crucial to develop analytical methods to interpret data in complex coastal systems (e.g. Boehme et al., 1998; Chierici et al., 2006), given the fact that our capacity to separate the biological signal from physical mixing is limited in dynamic coastal oceans. For instance, in recent studies the contribution from horizontal transports (mixing) was often not separated from other controlling processes (e.g. Schiettecatte et al., 2006; Shadwick et al., 2015) or was simply quantified on the basis of a constant linear relationship between dissolved inorganic carbon (which is biologically non-conservative) and salinity observed during cruises (e.g. Shadwick et al., 2011). Mixing could greatly influence the interpretation of the *in situ* biological signal occurring in shelf waters (Jiang et al., 2013; Wang et al., 2005), and thus this issue must be properly addressed.

The South Atlantic Bight (SAB) is a low- to mid-latitude continental shelf bordered by abundant salt-marshes to the west and by the Gulf Stream, a western Atlantic boundary current, to the east (Menzel, 1993). The SAB and its associated marsh-surrounded estuarine and nearshore areas have been a focus of coastal ocean air–sea CO_2 exchange studies over the past decades (Cai, 2011; Cai and Wang, 1998; Cai et al., 2003; Jiang et al., 2008a, 2008b, 2013; Signorini et al., 2013; Wang et al., 2005). Progress has been made in exploring the mechanism of pCO_2 variability and identifying the sink/source status with respect to atmospheric CO_2. Strong CO_2 outgassing in estuaries and inner shelf areas was attributed to direct transport of CO_2 from marshes and estuaries and to respiration of marsh-exported organic carbon (Cai et al., 1999; Cai and Wang, 1998; Jiang et al., 2008b, 2013; Wang et al., 2005). In the entire SAB temperature played a dominant role in seasonal variation of sea surface pCO_2 (Jiang et al., 2008a). More recently, Jiang et al. (2013) improved the mechanistic understanding of pCO_2 variability in the SAB based on seasonal cruise observations and identified the relative contributions of temperature, terrestrial inputs, and air–sea CO_2 exchange to pCO_2 variation.

Previous studies in the SAB were generally based on shipboard surveys and focused on mapping spatial distributions of pCO_2 using several cruises in an annual cycle (Jiang et al., 2008a, 2013; Wang et al., 2005). The result obtained during one cruise, a snapshot, was usually used to represent the state of two or more months. This can result in large uncertainties in air–sea CO_2 fluxes estimates and misinterpret controlling processes. For instance, during early studies Cai and coworkers inferred that the SAB was a CO_2 source to the atmosphere based on very limited cruise investigations along a cross-shelf transect (Cai et al., 2003; Wang et al., 2005). A more recent six-cruise whole shelf study showed that while the inner shelf was a source of CO_2 to the atmosphere, the combined shelf regions were actually a net CO_2 sink on an annual basis (Jiang et al., 2008a). The SAB has no annual spring bloom, but there are multiple small productive events throughout the year as a result of Gulf Stream eddies and meanders (Lee et al., 1991; Menzel, 1993) that can easily not be observed in limited surveys. The influence of these small productive events on pCO_2 has not been reported to date in the SAB.

In this study, we report the first full annual record of sea surface pCO_2 from 18 July 2006 through 31 October 2007 in the SAB and estimate air–sea CO_2 fluxes based on high-frequency (every three hours) observations from a buoy (Station 41008) located at Gray's Reef National Marine Sanctuary, Georgia, USA (Fig. 1). Our main focus is to present a 1-D time series pCO_2 model with multiple controlling processes and to evaluate its applicability at a seasonally varying dynamic site. We identify the major processes that control surface pCO_2 via both property regressions and model analysis. In addition, considering the high temporal variability of physical and biogeochemical processes in river-influenced coastal systems, we assess the influence of enhanced river inputs (decreased salinity) on seawater pCO_2 and potential limitations associated with shipboard surveys in estimating air–sea CO_2 fluxes and annual net community production (NCP) in dynamic coastal waters such as the SAB. In a follow-up work, we will extend the method presented here to all data since 2006 and further explore the impact of extreme events, interannual variation, and the secular trend at sub-decadal scale.

2. Site description and methods

2.1. Study site

The SAB is shallow (average depth of 28 m), and is divided into inner, middle, and outer shelf with boundaries at 20 m, 40 m, and 60 m depths extending from 27° to 35°N. It is generally warm (10–28 °C) with salinities ranging from 30 to 37 (Atkinson et al., 1983). There are many small rivers entering the SAB and extensive salt marshes between the barrier islands and the shorelines, the majority of which are located in the central SAB (between 31° and 33°N) (Menzel, 1993). The SAB receives a total annual river discharge of approximately 66 km^3 (2.7% of the SAB volume) (Menzel, 1993). The Altamaha River, one of the largest rivers along the US southeastern coast (Fig. 1) has an average annual discharge of 4.3–19.5 km^3 (U.S. Geological Survey, USGS) with the greatest discharge in February–April (Menzel, 1993). On the inner shelf circulation is largely driven by freshwater inputs, local wind, and tide forcing; on the middle shelf the influence from river discharge decreases and circulation is occasionally influenced by the Gulf Stream; and on the outer shelf circulation is primarily controlled by the Gulf Stream (Lee et al., 1991; Menzel, 1993).

On 17 July 2006, a moored autonomous pCO_2 ($MAPCO_2$) system (Willcox et al., 2010) was installed on a buoy (Station 41008, owned and maintained by the National Data Buoy Center, NDBC) located at the Gray's Reef National Marine Sanctuary (GRNMS, 31.402°N, 80.869°W, water depth 18.3 m), 74 km southeast of Savannah, Georgia, USA (Fig. 1). This location is roughly on the boundary between the inner and middle shelf of central SAB (Menzel, 1993). It can be representative of the inner shelf and experience strong terrestrial inputs during high river discharge; however, it may also represent the middle shelf during low discharge with limited river influences. Thus, this site provides us a good opportunity to examine both the terrestrial and oceanic influences on shelf biogeochemistry and carbon fluxes.

2.2. Time series monitoring

A suite of physical (sea surface temperature – SST, salinity – SSS, wind speed, and barometric pressure) and chemical parameters (CO_2 concentration or mole fraction in the water and air, and dissolved oxygen – DO) were continuously measured at the buoy site from 18 July 2006 through 31 October 2007 (http://pmel.

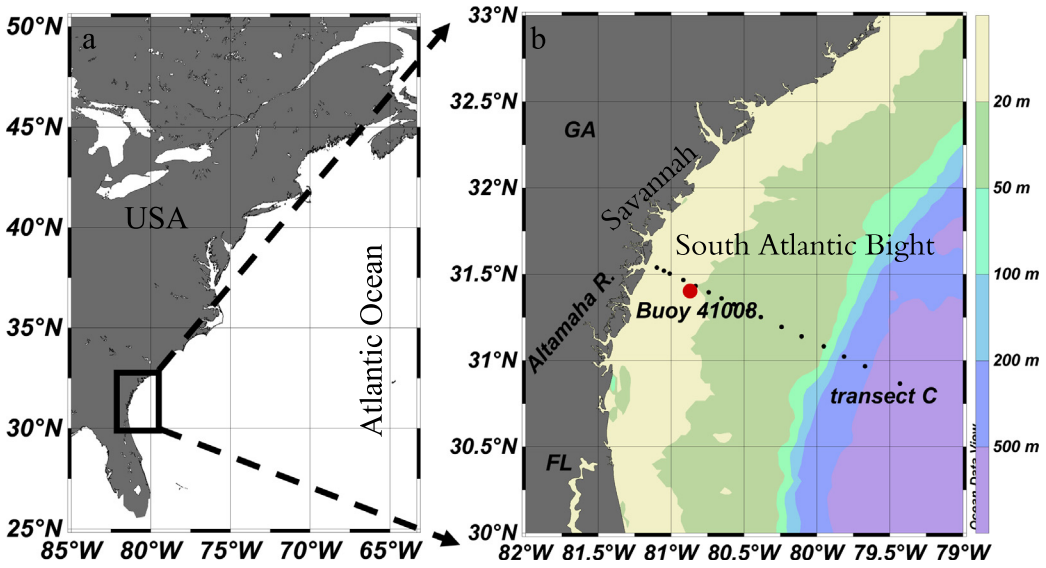

Fig. 1. Study area. (a) The location of the study area in the USA east coast (within the black box); (b) the location of buoy 41008 in the South Atlantic Bight (SAB). In (b), the black dots denotes the stations along transect C investigated by Jiang et al. (2008a) during 2005–2006, and the red dot represents the location of the buoy. (For interpretation of the references to color in this figure legend, the reader is referred to the web version of this article.)

noaa.gov/co2/story/Grays+Reef). Occasionally, during ground-truthing events, the frequency of data collection was increased to hourly or every 30 min. SST and SSS were measured every three hours using a Seabird Microcat C-T at a water depth of ~0.6 m. Data of the Altamaha River discharge (http://gce-lter.marsci.uga.edu/portal/usgs_doctortown/multiyear/data/index.xml) were used to explore the influence of river discharge on SSS. The Altamaha River discharge was recorded every 15 min at a USGS hydrological station in Doctortown, Georgia (31°39′16″N, 81°49′41″W). Hourly wind speed data at 5 m above sea level (measured by an RM Young anemometer) and hourly barometric pressure data at sea level (measured by a Serta barometer) from the buoy were used as well.

Overlying air and surface water pCO_2 were determined every three hours using a $MAPCO_2$ system (see Sutton et al. (2014b) for technical details). Briefly, CO_2 concentrations in the air, and in the air at equilibrium with sea surface water via a bubble type equilibrator were determined by a non-dispersive infrared analyzer (Licor 820). The Licor 820 was calibrated before every measurement with CO_2-free air (passing through a soda lime plug) and a ~500 ppm (parts per million) CO_2 standard traceable to World Meteorological Organization references prepared by NOAA's Earth System Research Laboratory (Sutton et al., 2014b). Both seawater and atmospheric CO_2 concentrations were converted to pCO_2 in 100% H_2O saturated air (as at sea surface) using the water vapor pressure of Weiss and Price (1980) and the atmospheric pressure as by Sutton et al. (2014b).

Uncertainty of the $MAPCO_2$ system was estimated to be ±2 μatm (Sutton et al., 2014b). We also measured surface water pCO_2 around the buoy on 20 June and 27 July 2007 (Fig. 2) using an underway CO_2 system (Licor-7000 infrared gas analyzer coupled to a gas–water equilibrator) similar to that described by Jiang et al. (2008a). During these two short cruises, mean underway pCO_2 and buoy pCO_2 agreed well (391 ± 1 μatm vs. 392 ± 3 μatm and 419 ± 4 μatm vs. 419 ± 5 μatm, respectively). More extensive underway measurements after this study period also showed consistent results with the buoy data (W.-J. Cai unpub.).

Atmospheric and surface seawater oxygen partial pressures were measured from the air intake and equilibrator using a motion stable galvanic cell oxygen sensor (MAX-250, Maxtec, Inc.). This was not a standard oceanographic method for measuring oxygen, and these data were primarily used as a diagnostic tool for the $MAPCO_2$ system. The O_2 saturation level (DO%) was calculated from the ratio of surface seawater to atmospheric oxygen partial pressures. DO content in surface water was then calculated from the DO% using the formula of oxygen solubility in seawater (Garcia and Gordon, 1992). Also one-day composite Aqua MODIS (Moderate Resolution Imaging Spectroradiometer) chlorophyll *a* (Chl *a*) data (from http://coastwatch.pfeg.noaa.gov/erddap/griddap/erdMEchla1day.graph) were used as a qualitative measure of biological activity. Although satellite Chl *a* data in the coastal ocean will be more affected by suspended solids compared with the open ocean, it can be used to roughly reflect biological activity in combination with DO% data.

2.3. Calculating air–sea CO_2 flux

Air–sea CO_2 flux, F_{CO2}, was calculated according to the bulk flux equation:

$$F_{CO2} = k \times K_0 \times (pCO_{2water} - pCO_{2air}) \quad (1)$$

where k is the gas transfer velocity; K_0 is the solubility coefficient of CO_2 (Weiss, 1974); and pCO_{2water} and pCO_{2air} are the pCO_2 in the surface water and the atmosphere, respectively. In this paper, a positive value of F_{CO2} denotes CO_2 releases from water to the atmosphere.

Gas transfer velocity, k, was estimated using the parameterization of the gas transfer velocity with wind speeds proposed by Wanninkhof (1992) and revised by Ho et al. (2006) and Sweeney et al. (2007) as expressed in Eq. (2).

$$k = 0.27 \times U_{10^2} \times (Sc/660)^{-0.5} \quad (2)$$

where U_{10} (m s^{-1}) is the wind speed at the height of 10 m above sea surface. Since our wind speed was measured at 5 m above sea surface, it was converted to U_{10} by multiplying a factor of 1.06 (Jiang et al., 2008a). Sc is the Schmidt number, which can be calculated after Wanninkhof (1992).

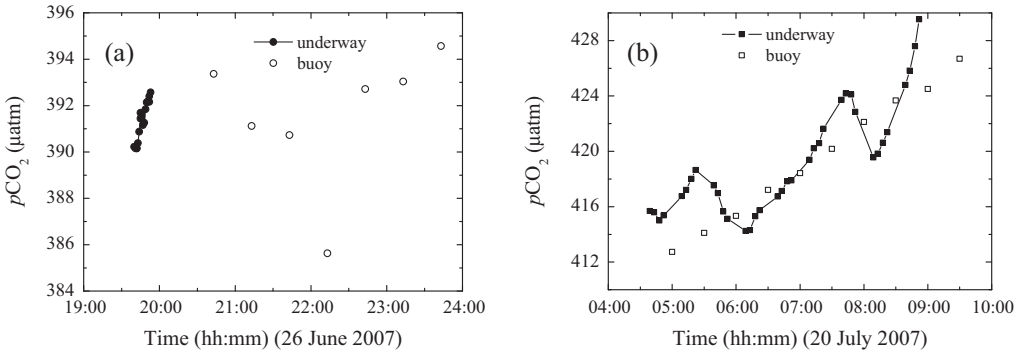

Fig. 2. Comparison of buoy pCO_2 and underway pCO_2 on 26 June 2007 (a) and 20 July 2007 (b), respectively. For comparison, underway CO_2 data on both days were selected from ±0.02° (~2 km) in longitude and latitude from the buoy. The MAPCO$_2$ system was set to measure more rapidly during these comparisons at 30 min intervals as opposed to the standard three hour intervals.

2.4. Determination of total alkalinity (TA) and dissolved inorganic carbon (DIC)

TA measurements were made in the central SAB primarily in 2005–2006 and less often in recent years. Some of these data have been published (Cai et al., 2010). Briefly, water samples were collected using a Conductivity, Temperature and Depth (CTD) rosette sampler, preserved with a saturated $HgCl_2$ solution and stored in borosilicate glass bottles. TA was measured by open cell Gran titration with a measurement precision of ±0.1% (Cai et al., 2010). Certified Reference Materials from A. Dickson of Scripps Institution of Oceanography were used during the analysis for reference and validation (Cai et al., 2010).

Considering the shallow water depth at the buoy site (Fig. 1), we only used the TA data in the upper 30 m along the C transect with a salinity range of 31.7–36.5 to derive the TA–salinity (S) relationship (Fig. 3). These data were collected from six cruises that covered all seasons, i.e. in January 2005, March 2005, July 2005, October 2005, December 2005, and May 2006 cruises (Jiang et al., 2008a). The relationship of TA and S is as follows:

$$TA = 49.66(\pm 0.83) \times S + 573.63(\pm 29.67) (r^2 = 0.93, n = 277, p < 0.001) \quad (3)$$

The uncertainty associated with TA was estimated from the residual values of the predicted alkalinity and was ~13 µmol kg^{-1} (<1%), larger than that in the Southern Ocean (5 µmol kg^{-1}, Shadwick et al., 2015), but similar to that in the Scotian Shelf region of the Canadian northwestern Atlantic Ocean (Shadwick et al., 2011). This TA and salinity relationship was very similar to that given by Cai et al. (2010) using a more extended database including those from deep waters (also see Fig. s1 in the supplementary materials). The relationship was robust, and was further validated by measured data around the buoy from the U.S. Gulf of Mexico and East Coast Cruise (GOMECC) in 2007 and from a buoy maintenance cruise in 2008 (Fig. 3).

Subsequently, high temporal-resolution TA values (three-hourly) at the buoy site were calculated using the buoy salinity data based on the conservative behavior of TA in the SAB (Fig. 3, except in the very nearshore area with salinity <30) as revealed by Wang et al. (2005) and Cai et al. (2010). While contributions of other acid–base species such as organic matter could be important within the estuaries, they were negligible in offshore surface waters (Cai et al., 1998). Then, we calculated high-resolution DIC concentrations at the buoy site based on the salinity-derived TA and sea surface pCO_2 data using the program CO2SYS (Lewis and Wallace, 1998) according to the equilibrium constants of Mehrbach et al. (1973) refit by Dickson and Millero (1987).

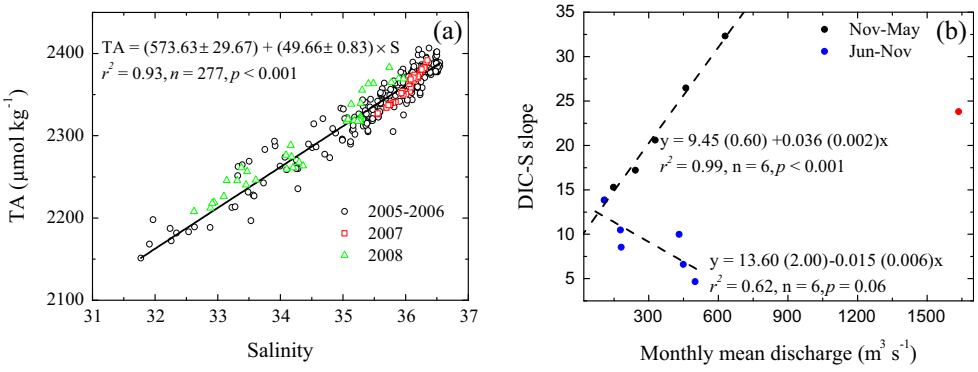

Fig. 3. Relationship between total alkalinity (TA) and salinity (S) (a) and relationship between DIC–salinity slope values and monthly mean discharge of Altamaha River (b). The TA–S relationship was determined from six cruises covering all seasons, i.e., January 2005, March 2005, July 2005, October 2005, December 2005, and May 2006 (black circle) and validated using the measured data along transect C during the GOMECC GA cruise in July 2007 (red square, see Cai et al. (2010)) as well as in August and December 2008 near the buoy (green triangle). Note that only the data with the salinity range of 31.7–36.7 (buoy salinity range) in the upper 30 m were used to build the TA–S relationship. In (b), the DIC–salinity slope values were calculated from the monthly varying DIC values at the nearshore and open ocean end-members determined by Jiang et al. (2013) (see their Table 1). Considering that only the slopes in January, March, May, July, and October were provided, slope values in other months were obtained by linear interpolation (Fig. s4 in the supplementary materials). In addition, data in April (red dot) was not considered during the linear regression due to extremely high river discharge of 1636 m^3 s^{-1}. The Altamaha River discharge data recorded at a USGS hydrological station in Doctortown, Georgia (31°39′16″N, 81°49′41″W) are from http://gce-lter.marsci.uga.edu/portal/usgs_doctortown/multiyear/data/index.xml. (For interpretation of the references to color in this figure legend, the reader is referred to the web version of this article.)

2.5. A 1-D mass budget model for separating pCO_2 controlling processes

To determine the contribution of temperature, air–sea exchange, mixing, and biological activity to pCO_2 variability, we developed a simple 1-D mass budget model similar to that of Boehme et al. (1998). We first set the starting time as time t_1, at which SST, SSS, and carbonate parameters (DIC, TA, and pCO_2) were T_1, S_1, TA_1, DIC_1 and $(pCO_2)_1$, respectively. Then after a time increment to time t_2, these parameters changed to T_2, S_2, TA_2, DIC_2, and $(pCO_2)_2$. In the following calculations, subscripts "tem", "a–s", "mix", and "bio" denote temperature, air–sea exchange, mixing, and *in situ* biological activity, respectively; and the sign "Δ" denotes the change of a parameter during the time step. For example, "ΔpCO_{2tem}" denotes pCO_2 change caused by temperature change between time 2 and time 1.

Total pCO_2 change (ΔpCO_2) from t_1 to t_2 caused by a combination of pCO_2 controlling processes can be expressed by Eq. (4a). Similarly, changes in both DIC and TA can be expressed in Eqs. (4b) and (4c). Note that changes in carbonate parameters caused by calcium carbonate dissolution/precipitation were neglected in our calculation given the conservative behavior of TA in this area (Fig. 3).

$$\begin{aligned}\Delta pCO_2 &= (pCO_2)_2 - (pCO_2)_1 \\ &= \Delta pCO_{2tem} + \Delta pCO_{2a-s} + \Delta pCO_{2mix} + \Delta pCO_{2bio} \\ &\quad + \Delta pCO_{2non}\end{aligned} \tag{4a}$$

$$\Delta DIC = \Delta DIC_{a-s} + \Delta DIC_{mix} + \Delta DIC_{bio} \tag{4b}$$

$$\Delta TA = \Delta TA_{mix} + (-17/106 * \Delta DIC_{bio}) \tag{4c}$$

where ΔpCO_{2non} is a non-linear term, the difference between ΔpCO_2 and the sum of pCO_2 change due to each process, considering that pCO_2 response to SST or DIC changes is not linear. Note that while on a short time scale (three-hourly or daily), the non-linear term is essentially zero, a small but noticeable non-linear term appears as we used a monthly time scale for the mixing and biological terms (see below). Here ($-17/106 * \Delta DIC_{bio}$) is the expected TA change during biological use or release of DIC if the Redfield ratio is assumed (Redfield et al., 1963). In practice we ignored the biological term in Eq. (4c), because: (1) it is expected to be rather small as TA and salinity show a conservative relationship, and (2) in the current approach we take the biological term to close the budget (i.e., it is estimated as the remainder of the other terms).

Each of the four different contributing factors in Eq. (4) can be determined through the following steps:

2.5.1. Temperature

We used the pCO_2 temperature dependence coefficient (0.0423) proposed by Takahashi et al. (1993) to calculate the thermal effect. The result is the same for calculating temperature effect on a three-hour or monthly time scale.

$$\Delta pCO_{2tem} = (pCO_2)_1 \times \exp(0.0423 \times (T_2 - T_1)) - (pCO_2)_1 \tag{5}$$

Therefore, the three subsequent processes (air–sea exchange, mixing, and biological activity) during each time step ($t_2 - t_1$) were dealt with under isothermal conditions.

2.5.2. Air–sea exchange

Air–sea CO_2 exchange changes DIC, but not TA.

$$\Delta DIC_{a-s} = -F \times (t_2 - t_1)/(D \times H) \tag{6a}$$

$$(DIC_2)_{a-s} = DIC_1 + \Delta DIC_{a-s} \tag{6b}$$

$$\Delta pCO_{2a-s} = f((DIC_2)_{a-s}, TA_1, S_1, T_1) - (pCO_2)_1, \tag{6c}$$

where F is the air–sea CO_2 flux (see Section 2.3); D is the seawater density (kg m^{-3}); and H is the mixed layer depth. From October to May, it is assumed that the mixed layer extends to the bottom (H is 18 m). In July however, H is reduced to 8 m (Fig. s2 in the supplementary materials), and in September and June to 13 m (the mean between the depth in October–May and the depth in July); $(DIC_2)_{a-s}$ is the predicted DIC at time t_2 due solely to air–sea exchange from time t_1 to t_2; f(DIC, TA, S, T) denoted the pCO_2 as a function of DIC and TA at a given temperature and salinity and was calculated using the program CO2SYS (Lewis and Wallace, 1998) according to the equilibrium constants of Mehrbach et al. (1973) refit by Dickson and Millero (1987). A three-hour time scale was applied in the calculation of air–sea flux, which was also aggregated into monthly time scale for presentation and for subsequent calculations (see below).

2.5.3. Mixing

We attributed salinity changes solely to nearshore and open-ocean mixing (horizontal mixing), neglecting the other processes including evaporation and precipitation. As salinity is the only parameter characterizing mixing, our mixing term in fact should include both horizontal and vertical mixing. However, due to the shallowness of the site, in reality, horizontal water movement should be the dominant form of mixing, except for mixed layer deepening in September. In addition, at this site and its immediate seaward stations, even during July (the stratified time), bottom water DIC values, together with the surface water DIC values were located on the same DIC–salinity line (Figs. s1–s3). Thus, salinity alone is adequate to measure both horizontal and vertical mixing (and they are not differentiated hereafter). Using the linear relationship of mixing between a low salinity end-member and the seawater end-member (Friis et al., 2003), we obtained the DIC change due to mixing (ΔDIC_{mix}) during time interval ($t_2 - t_1$) (Eq. (7a)).

$$\Delta DIC_{mix} = (DIC_{oce} - DIC_{ns})/(S_{oce} - S_{ns}) \times (S_2 - S_1) \tag{7a}$$

$$(DIC_2)_{mix} = DIC_1 + \Delta DIC_{mix} \tag{7b}$$

where DIC_{oce} and DIC_{ns} are DIC at the ocean and nearshore end-members, respectively; S_{oce} and S_{ns} are salinity at the ocean and at nearshore end-members, respectively; and S_2 and S_1 are salinity at time t_2 and t_1, respectively. $(DIC_2)_{mix}$ is the predicted DIC at time t_2 due to mixing from time t_1 to t_2. For the calculations, we use the slope of the DIC–salinity relationship, i.e., $(DIC_{oce} - DIC_{ns})/(S_{oce} - S_{ns})$. We used the monthly varying DIC values at the nearshore and open ocean end-members determined by Jiang et al. (2013) to calculate the slope (see their Table 1). Considering that only the slopes in January, March, May, July, and October were provided, slope values in other months were obtained by linear interpolation (Fig. s4 in the supplementary materials). During the months of November to May, the slope value presented a very good positive relationship with monthly mean discharge of Altamaha River, whereas during the months of June to October, the slope value presented a negative relationship with river discharge (Fig. 3b). In this work, we obtained the monthly slope value during our buoy data period (2006–2007) using the relationships shown in Fig. 3b (see more details in Fig. s4) and quantified the contribution of mixing to monthly pCO_2 changes. Monthly changes were defined here as the difference of the parameters between the first day and the last day in each month.

TA changes due to mixing can be estimated directly from the TA–S relationship (Fig. 3).

$$\Delta TA_{mix} = 49.66 \times (S_2 - S_1) \tag{7c}$$

Table 1
Surface water properties (sea surface salinity (SSS), temperature (SST, °C), dissolved oxygen saturation level (DO%), surface pCO_2 (μatm) and temperature normalized pCO_2 ($npCO_2$, μatm)), atmospheric pCO_2 (μatm), wind speed at the height of 10 m above sea surface (U_{10}, ms^{-1}), and air–sea CO_2 flux (Flux, mmol m^{-2} d^{-1}) during September and October of 2006 and 2007. Values in the table are in the form of mean ± one standard deviation.

Period	SSS	SST	DO%	Surface pCO_2	Surface $npCO_2$	Atmospheric pCO_2	U_{10}	Flux
September 2006	36.24 ± 0.09	28.29 ± 0.78	98.31 ± 0.83	393 ± 14	317 ± 9	367 ± 5	5.70 ± 2.60	2.08 ± 2.35
September 2007	35.58 ± 0.43	28.02 ± 0.90	99.04 ± 1.00	427 ± 17	350 ± 24	368 ± 5	4.75 ± 2.72	3.42 ± 3.25
October 2006	36.26 ± 0.10	24.75 ± 1.63	98.88 ± 0.48	353 ± 25	330 ± 6	374 ± 6	5.90 ± 2.82	−2.18 ± 4.31
October 2007	34.86 ± 0.15	25.44 ± 0.76	98.56 ± 0.73	414 ± 12	378 ± 10	373 ± 6	5.32 ± 2.29	2.84 ± 2.30

$$(TA_2)_{mix} = TA_1 + \Delta TA_{mix} \quad (7d)$$

where $(TA_2)_{mix}$ is the predicted TA at time t_2 due only to mixing from time t_1 to t_2.

We then obtained the ΔpCO_{2mix}:

$$\Delta pCO_{2mix} = f((DIC_2)_{mix}, (TA_2)_{mix}, S_2, T_1) - (pCO_2)_1 \quad (7e)$$

2.5.4. Biology

We assigned the rest of DIC changes to biological processes to close the budget.

Thus,

$$\Delta DIC_{bio} = \Delta DIC - (\Delta DIC_{a-s} + \Delta DIC_{mix}) \quad (8a)$$

$$(DIC_2)_{bio} = DIC_1 + \Delta DIC_{bio} \quad (8b)$$

where $(DIC_2)_{bio}$ is the predicted DIC at time t_2 only due to biological activity from time t_1 to t_2.

We then obtained ΔpCO_{2bio} in Eq. (8c):

$$\Delta pCO_{2bio} = f((DIC_2)_{bio}, TA_1, S_1, T_1) - (pCO_2)_1 \quad (8c)$$

Also, by definition, we derived NCP:

$$NCP = -\Delta DIC_{bio} \times H/(t_2 - t_1) \quad (8d)$$

3. Results

3.1. Hydrographic data

SST at the buoy site showed large seasonal variations, with the highest value of 29–31 °C in the summer (July–August) of 2006 and 2007, and the lowest value of ~12 °C in the winter (February 2007) (Fig. 4a). SSS exhibited high values (>36) between mid-July and November 2006, and low values (<35) between mid-February and June 2007 (Fig. 4b). SSS was particularly low during February–April 2007 and showed large fluctuations (Fig. 4b). SSS and Altamaha River discharge showed a negative relationship ($r = -0.62$, $p < 0.05$, $n = 455$) after considering a lag time of up to 42 days (Fig. s5 in the supplementary materials). SSS thus can be used as a proxy for the influence of river inputs to the buoy site because local precipitation/evaporation events do not have a direct or strong influence at this site (unpublished data). Mean SSS was lower during September–October 2007 than September–October 2006 (Fig. 4b and Table 1). Vertically observations show that the water column was well mixed throughout most of a year, except in summer (July 2005) (Fig. s2 in the supplementary materials).

3.2. Dissolved oxygen and chlorophyll a

During September 2006–February 2007, DO was slightly undersaturated with respect to the atmosphere, and exhibited small fluctuations (Fig. 4c). In contrast, there were large short-term fluctuations in DO% between 95% and 109% during April–September 2007 when several peaks of DO% occurred (Fig. 4c). Some peaks in DO% coincidently corresponded to Chl *a* peaks (Fig. 4c). Particularly between late April and early May 2007, a DO% peak of 109% and a Chl *a* peak of 9.5 mg m^{-3} were concurrently observed, indicting the occurrence of a bloom.

3.3. Atmospheric and sea surface pCO_2, TA, and DIC

The average atmospheric pCO_2 during the study period was 377 ± 10 μatm, with slightly lower values observed in May–October and higher values in November–April (Fig. 4a). In contrast, seawater pCO_2 showed large temporal variations (Fig. 4a). The average surface water pCO_2 was 373 ± 52 μatm, with values greater than 400 μatm in July–August and values less than 330 μatm in November–February. The highest seawater pCO_2 of 507 μatm was observed in August 2007 and the lowest value of 233 μatm in early May 2007 (Fig. 4a). In general, surface pCO_2 was undersaturated in cold months (November–March) with respect to the atmosphere and oversaturated in warm months (April–October) (Figs. 4a and 5a). This seasonal pattern of buoy pCO_2 in 2006–2007 was generally consistent with underway observations made during several cruises in 2005–2006 around this buoy location, although underway surface pCO_2 values in summer 2005 and spring 2006 were somewhat higher than buoy CO_2 values in summer 2006 and spring 2007 (Fig. 4a, blue points). Compared with previous ship-based surveys, however, very low pCO_2 of 233–290 μatm between April and June 2007 was observed by the high temporal resolution monitoring of the buoy (Fig. 4a), possibly associated with biological production as indicated by high DO% and Chl *a* values (Fig. 4c). Furthermore, mean surface pCO_2 was higher in September–October 2007 than in the same period of 2006 (Fig. 4a and Table 1).

To remove the temperature effect on pCO_2, we normalized pCO_2 to a constant temperature of 23.24 °C (the mean temperature during the study period) following the approach of Takahashi et al. (1993). The temperature normalized pCO_2 ($npCO_2$) reflects pCO_2 variability due to non-temperature factors such as mixing, air–sea exchange and biological activity (e.g. Körtzinger et al., 2008; Xue et al., 2012). We found that $npCO_2$ also had a wide range of 230–500 μatm, with higher values in cold months and lower values in warm months (Fig. 4a).

As described in Section 2.4 TA and DIC at the buoy site were estimated (Fig. 4d). By definition TA strictly followed SSS variabiltiy, with high values corresponding to high salinity values and vice versa. Estimated DIC was high from December 2006 to February 2007 and the lowest DIC values occurred during April–June 2007 due to the occurrence of biological production events (Fig. 4).

3.4. Air–sea CO_2 flux and NCP

Air–sea CO_2 fluxes at this site showed great temporal variability on different timescales (Fig. 5). Especially during October–December 2006, every three-hour (black line) or one-day averaged (green line) air–sea CO_2 fluxes varied from −20 to −5 mmol m^{-2} d^{-1} within several hours or days due mainly to the frequent occurrence of high wind speed greater than 10 m s^{-1} (Fig. 5b). The study site even switched rapidly between being a CO_2 source and sink within a few days during October 2006 and April–June 2007. There was

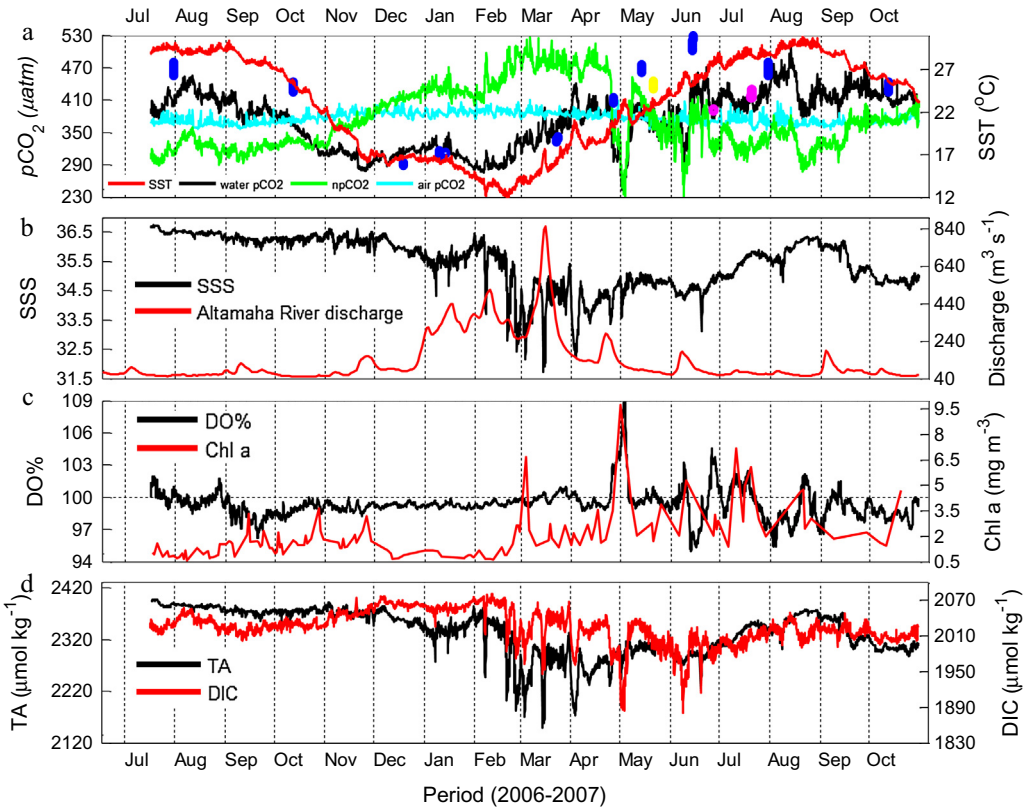

Fig. 4. Time series of sea surface pCO_2 (black), temperature normalized pCO_2 ($npCO_2$, green), atmospheric pCO_2 (cyan), and sea surface temperature (SST, red) (a), sea surface salinity (SSS, black) and Altamaha River discharge (red) (b), dissolved oxygen saturation level (DO%, black) and one-day composite Aqua MODIS chlorophyll a (Chl *a*, red) (c), and total alkalinity (TA, black) estimated by TA–*S* relationship and dissolved inorganic carbon (DIC) calculated from estimated TA and sea surface pCO_2 (d) from 18 July 2006 through 31 October 2007. In addition, the cruise pCO_2 data from January, March, April, May, June, July, October and December 2005 (in blue), May 2006 (in yellow) and June and July 2007 (in magenta, also shown in Fig. 2) were also shown. For comparison, underway CO_2 data from January, March, July, October, and December 2005, and May 2006, which are from Jiang et al. (2008a), are used from ±0.05° (~5 km) in longitude and latitude from the buoy. Data shown in this figure in April, May, and June 2005 are 0.15 (~15 km), 0.1 (~10 km) and 0.3 (~30 km) degrees in longitude and latitude from the buoy, respectively. CO_2 data in June and July 2007 are selected from ±0.02° (~2 km) in longitude and latitude from the buoy.

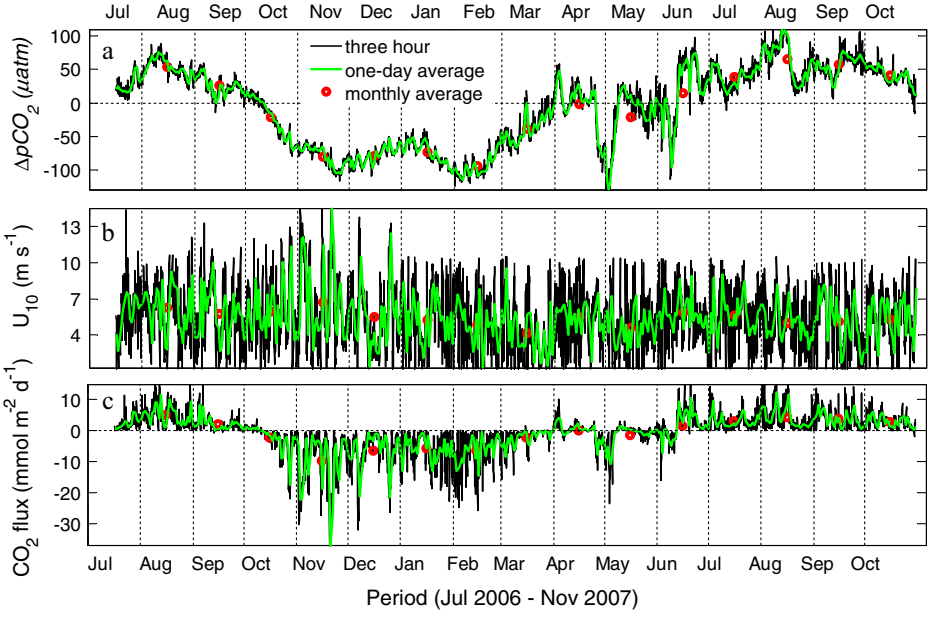

Fig. 5. Time series of pCO_2 difference between the ocean and the atmosphere ($\Delta pCO_2 = pCO_{2water} - pCO_{2air}$, a), wind speed at height of 10 m above sea surface (U_{10}, b), and air–sea CO_2 flux (c) from 18 July 2006 through 31 October 2007. The black line, green line, and the red circles denote every three hour, one-day averaged and monthly averaged data, respectively. (For interpretation of the references to color in this figure legend, the reader is referred to the web version of this article.)

Table 2
Monthly changes in dissolved inorganic carbon (ΔDIC), its components due to various processes, salinity (Δ*S*), and NCP. Components of DIC changes include air–sea exchange (ΔDIC_{as}), mixing (ΔDIC_{mix}), and biological activity (ΔDIC_{bio}). ΔDIC is the difference of DIC between the first day and the last day in each month; positive (or negative) values denote the increase (or decrease) during each month. Unit of ΔDIC and NCP is in μmol kg^{-1} and mmol m^{-2} d^{-1}, respectively. Uncertainties associated with monthly DIC changes and NCP are presented in the parenthesis.

Month	ΔDIC	ΔDIC_{as}	ΔDIC_{mix}	ΔDIC_{bio}	NCP	Δ*S*
July 2006	3.4 (18.4)	−4.1 (1.0)	−1.7 (0.4)	9.2 (18.4)	−4.3 (8.7)	−0.13
August 2006	−0.6 (18.4)	−19.2 (4.8)	−2.3 (0.5)	21.0 (19.0)	−5.6 (5.1)	−0.18
September 2006	10.3 (18.4)	−7.6 (1.9)	0.4 (0.1)	17.5 (18.5)	−7.8 (8.4)	0.04
October 2006	0.3 (18.4)	3.7 (0.9)	−0.5 (0.1)	−2.9 (18.4)	1.7 (11.0)	−0.04
November 2006	30.9 (18.4)	15.9 (4.0)	−0.3 (<0.1)	15.3 (18.8)	−9.5 (11.8)	−0.02
December 2006	10.4 (18.4)	10.6 (2.6)	−2.1 (0.1)	2.0 (18.6)	−1.2 (11.1)	−0.16
January 2007	9.9 (18.4)	9.6 (2.4)	12.7 (0.4)	−12.5 (18.5)	7.5 (11.2)	0.59
February 2007	−92.9 (18.4)	9.7 (2.4)	−80.8 (2.4)	−21.9 (18.7)	14.6 (12.7)	−3.54
March 2007	49.5 (18.4)	3.8 (0.9)	41.4 (1.2)	4.4 (18.4)	−2.6 (11.1)	1.71
April 2007	−78.4 (18.4)	−0.1 (0.1)	−6.6 (0.2)	−71.7 (18.4)	44.5 (13.2)	−0.42
May 2007	11.7 (18.4)	2.4 (0.6)	−0.5 (<0.1)	9.7 (18.4)	−5.8 (11.1)	−0.04
June 2007	−9.2 (18.4)	−6.4 (1.6)	0.7 (0.2)	−3.5 (18.5)	1.6 (8.3)	0.06
July 2007	13.5 (18.4)	−11.5 (2.9)	6.4 (1.5)	18.6 (18.7)	−5.0 (5.0)	0.51
August 2007	11.6 (18.4)	−16.2 (4.1)	7.6 (1.7)	20.2 (18.9)	−5.4 (5.1)	0.60
September 2007	11.2 (18.4)	−12.9 (3.2)	−9.6 (2.2)	33.8 (18.8)	−15.1 (8.7)	−0.79
October 2007	0.8 (18.4)	−10.3 (2.6)	−4.0 (0.9)	15.1 (18.6)	−9.1 (11.2)	−0.32

also obvious monthly and seasonal variability (Fig. 5). During July–September 2006 the sea to air CO_2 flux ranged from <1 to ~9 mmol m^{-2} d^{-1}, representing a CO_2 source to the atmosphere, while the study site was a CO_2 sink during most of the time between October 2006 and mid-June 2007. In addition, air–sea CO_2 flux in September–October 2006 was different from that in the same calendar months of 2007 (Fig. 5c and Table 1). For example, in October this site was a CO_2 sink in 2006 and a CO_2 source in 2007 (Fig. 5 and Table 1). Overall, the buoy site was a net CO_2 sink with respect to the atmosphere (−0.65 mol m^{-2} yr^{-1} during 18 July 2006–18 July 2007, or −0.43 mol m^{-2} yr^{-1} 4 during 31 October 2006–31 October 2007).

Monthly mean NCP in the mixed layer is listed in Table 2. During July–September of 2006 and 2007 there were negative NCP values, meaning that this site was heterotrophic, while during January to June 2007 there were either positive or near zero NCP values, meaning it was autotrophic or nearly at a metabolic balance. These results were in general agreement with Jiang et al. (2013)'s inference. In particular, a high NCP of 44.5 mmol m^{-2} d^{-1} was observed during April 2007 when a bloom occurred resulting in high DO% and high Chl *a* levels (Fig. 4c). Integrating the monthly NCP (Table 2), we found that this site was autotrophic on an annual basis with NCP varying from 0.44 mol m^{-2} yr^{-1} (November 2006–October 2007) to 0.99 mol m^{-2} yr^{-1} (September 2006–August 2007). NCP during September–October 2006 was also different from that in 2007 (Table 2). For example, NCP was positive (1.7 mmol m^{-2} d^{-1}) in October 2006 and negative in October 2007 (−9.1 mmol m^{-2} d^{-1}).

4. Discussion

4.1. Controlling processes of surface pCO_2 based on property regressions

Sea surface pCO_2 and SST showed strong positive relationships on an annual basis (r^2 = 0.64) and on monthly basis in most months (Fig. 6a and Table 3). Thus, SST played a dominant role in pCO_2 seasonal variations and could explain a majority of pCO_2 variability. This seasonal cycle feature was particularly clear during the cooling period from September 2006 to February 2007 and the warming period from late February to early April 2007 (Figs. 4 and 6). These results were consistent with previous findings in this region (Jiang et al., 2008a). However, it was also clear that gas exchange, mixing, and biology altered the carbonate chemistry in this open system at the buoy site over the annual cycle, which led to multiple pCO_2–SST evolving paths (rather than along one path predicted by Eq. (5) in a closed system). Deterioration or complete breakdown of pCO_2–SST relationships occurred on various occasions (Fig. 6a and Table 3). For example, sea surface pCO_2 increased with SST as predicted during the warming period from late February to April 2007, which was followed by lower and sharply changing pCO_2 between April and June 2007 (Fig. 6a). This behavior was very likely associated with high biological production and subsequent respiration as illustrated by high DO% and subsequent rapid decay of the signal (Fig. 4c). Therefore, episodic biological events had a strong impact on pCO_2 even though it is assumed that SST would be the most influential control on variability. In addition, the positive pCO_2-temperature relationship completely deteriorated during the peak winter period of February 2007 and peak summer period (July–August) of 2006 and 2007 (Fig. 6a and Table 3). Thus, despite the dominant role of SST in the annual cycle of pCO_2 variation, other factors also influenced pCO_2.

Sea surface npCO_2 and SSS showed significant, yet weaker, negative relationships than pCO_2-SST on an annual basis (r^2 = 0.36) and occasionally on monthly basis (Fig. 6b and Table 3). Thus, SSS variability, or river inputs, also played an important role in the annual cycle of pCO_2 aside from SST (Fig. s5 in the supplementary materials). Rivers transported terrestial carbon and CO_2 produced in the salt-marshes and within the estuaries to the shelf (Jiang et al., 2008b, 2013; Wang and Cai, 2004), which to a large extent explained the relatively high npCO_2 during low SSS in February–April 2007 and low npCO_2 during high SSS in summer (July–August) (Fig. 4). Negative relationships between npCO_2 and SSS also broke down on some occasions, for example, during April–June 2007 when biological production was episodically high (Figs. 6b and 4c). On monthly scales, surface npCO_2 and SSS showed strong negative relationships during the wet season in December 2006–April 2007 and the dry summertime (July–August) (Fig. 6b and Table 3). For instance, in February 2007 when an increase in pCO_2 of 48 μatm occurred together with a decrease in SSS of 3.54, we observed a strong negative relationship between npCO_2 and SSS with r^2 = 0.86 (Fig. 6b and Table 3), indicating that pCO_2 increase was likely associated with river inputs. While no relationship was observed between SSS and local precipitation at the buoy site and that the estimated SSS change was <0.05 units due to impact of daily rain events (data not presented), extreme precipitation events could have an impact on SSS and pCO_2 data. We defer a discussion of this issue to future examination of the entire dataset from 2006 through the present.

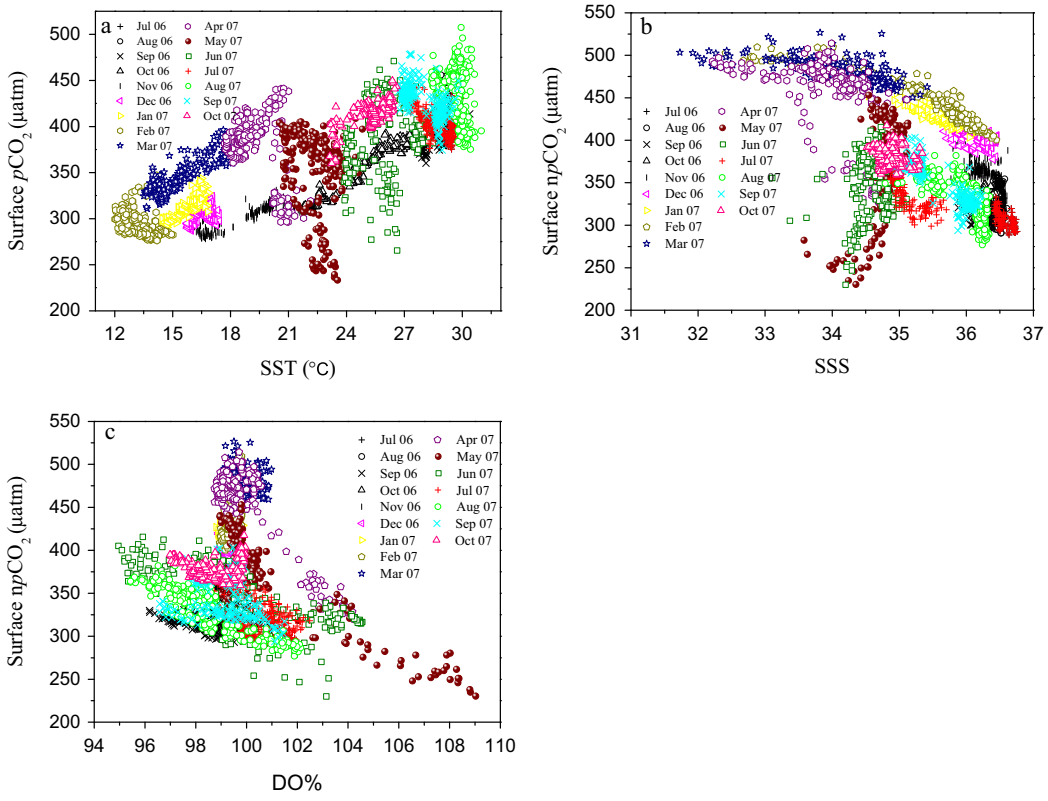

Fig. 6. Property–property plots of pCO_2 versus SST (a), temperature normalized $npCO_2$ (or $npCO_2$) versus SSS (b), and $npCO_2$ versus DO% (c). Regression results for each month can be found in Table 3.

Table 3
Regression results for pCO_2-SST, $npCO_2$-SSS, and $npCO_2$-DO% in each month from July 2006 to October 2007. The plots of pCO_2-SST, $npCO_2$-SSS, and $npCO_2$-DO% are shown in Fig. 6. *n* is the number of observations in each month.

Month	*n*	pCO_2-SST		$npCO_2$-SSS		$npCO_2$-DO%	
		r^2	*p*	r^2	*p*	r^2	*p*
July 2006	106	0.18	<0.001	0.38	<0.001	0.37	<0.001
August 2006	246	0.11	<0.001	0.55	<0.001	0.79	<0.001
September 2006	230	0.42	<0.001	0.03	<0.05	0.20	<0.001
October 2006	227	0.94	<0.001	–	ns	0.12	<0.001
November 2006	224	0.71	<0.001	0.22	<0.001	0.14	<0.001
December 2006	238	0.10	<0.001	0.58	<0.001	0.03	<0.05
January 2007	215	0.77	<0.001	0.72	<0.001	0.22	<0.001
February 2007	213	0.03	<0.05	0.86	<0.001	0.42	<0.001
March 2007	217	0.71	<0.001	0.45	<0.001	0.09	<0.001
April 2007	215	0.11	<0.001	0.23	<0.001	0.80	<0.001
May 2007	218	0.07	<0.001	0.34	<0.001	0.69	<0.001
June 2007	226	0.03	<0.05	–	ns	0.49	<0.001
July 2007	242	0.27	<0.001	0.60	<0.001	0.28	<0.001
August 2007	246	0.11	<0.001	0.55	<0.001	0.79	<0.001
September 2007	257	0.35	<0.001	0.76	<0.001	0.05	<0.001
October 2007	244	0.43	<0.001	–	ns	–	ns
All data	3581	0.64	<0.001	0.36	<0.001	0.02	<0.001

ns means "not significant" ($p > 0.05$).

As demonstrated by $npCO_2$ and DO% ($r^2 < 0.1$, Fig. 6c and Table 3), the role of biological activity in the annual cycle of pCO_2 was relatively weak compared with SST and SSS. Surface $npCO_2$ and DO%, however, showed strong negative relationships during spring and summer months (April–August) (Fig. 6c and Table 3), suggesting important influences of biological activity on surface pCO_2 during these periods. For example, during April–May 2007 when a bloom occurred as reflected by Chl *a* level and DO% (Fig. 4c), $npCO_2$ and DO% showed strong negative relationships (Table 3). This bloom began in late April, peaked in early May, and almost disappeared by late May. During this period, surface water pCO_2 followed the evolution of the bloom (Fig. 4), reflecting the dominance of biological activity on pCO_2. From the onset to the peak of the bloom (i.e., from late April to early May), surface pCO_2 decreased by ~150 µatm and reached a minimum of 233 µatm (the lowest observed value during the study period) (Fig. 4). While in August of both 2006 and 2007 we observed high pCO_2 values, as well as a strong negative relationship between $npCO_2$ and DO% ($r^2 = 0.79$), implying the possible influence of respiration (Fig. 6c and Table 3).

Overall although SST explains the main feature of the annual cycle and the dominant seasonal pattern of sea surface pCO_2, other non-thermal factors such as river inputs and biological activity are also important as suggested by the relationships of $npCO_2$ with DO % and SSS (Fig. 6 and Table 3). However, it is difficult to quantitatively identify the relative importance of these processes to pCO_2 variations based on property regressions alone due to their interactions (especially the river input and biological signals), which will be discussed further in Section 4.2.

4.2. Processes influencing monthly pCO_2 variability revealed by the 1-D model

4.2.1. Quantitative identification of pCO_2 controls

Contribution and relative importance of each driving factor to monthly DIC and pCO_2 variability are shown in Table 2 and Fig. 7. While the conclusions derived from the 1-D model are in general agreement with those derived from the property regressions, at times, they also illustrate how various processes enhance or cancel out each other. SST played an important role in pCO_2 variability during rapid cooling from September to November 2006

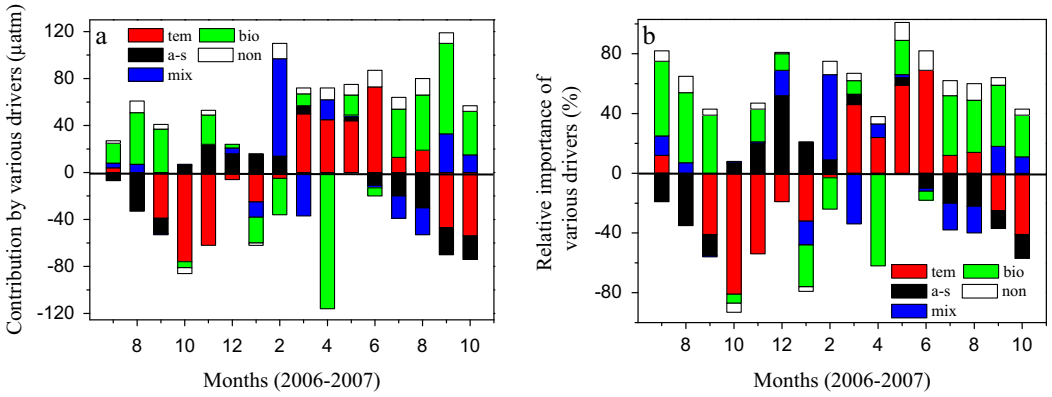

Fig. 7. Contribution (a) and relative importance (b) of temperature, ΔpCO_{2tem}, air–sea exchange, ΔpCO_{2a-s}, mixing, ΔpCO_{2mix} and biological activity, ΔpCO_{2bio} to pCO_2 changes as well as the non-linear term, ΔpCO_{2non} in each month during 2006–2007. The relative contribution was calculated as: $100 \times Xi/\sum_{i=1}^{5}|Xi|$. *Xi* is the pCO_2 change due to one process (the non-linear term included). Positive values denote the pCO_2 increase.

and during warming from March to June 2007 (Fig. 7). During September–November 2006 monthly pCO_2 decrease was 39–76 μatm due to cooling (Fig. 7b), and during March–June 2007 monthly pCO_2 increase was 44–73 μatm due to warming. SST changes during the rapid cooling or warming periods could account for most of the seasonal variability in pCO_2 between winter and summer, and thus SST was the most important factor of pCO_2 seasonal variation. In contrast, during the peak winter period in December–February and the peak summer period in July–August, the temperature effect was weak (less than 25 μatm, Fig. 7a).

Mixing between nearshore and open-ocean waters (primarily due to horizontal advection), characterized by salinity changes, had an important influence on pCO_2 variability, mainly during January–April and July–October 2007 with monthly SSS changes larger than 0.32 (Fig. 7 and Table 2). During these periods, monthly pCO_2 changes were 13–83 μatm due to mixing (Fig. 7a). This effect was especially notable in February 2007 when SSS decreased by 3.54 due to increased river inputs and thus pCO_2 increased by 83 μatm due to mixing with CO_2 rich nearshore waters. While in August 2007, SSS increased by 0.60, resulting in a pCO_2 decrease of 23 μatm due to mixing with open ocean waters.

Biological activity also played an important role in monthly pCO_2 variations (Fig. 7). During August–September 2006 and July–October 2007 monthly pCO_2 increase was 37–77 μatm due to biological respiration, while in January and February 2007 monthly pCO_2 decrease was 22–31 μatm due to biological production. Particularly during the bloom period in April 2007 pCO_2 decreased by 116 μatm due to strong photosynthetic uptake of CO_2 (Fig. 4c). While biological production was still strong in early May, it began to decay and disappeared at the end of May with the overall biological effect of increasing pCO_2 on a monthly scale.

Finally, the effect of air–sea exchange was relatively minor when compared with the influence of SST, mixing, and biological activity on pCO_2 (Fig. 7). The maximum monthly pCO_2 decrease was 20–32 μatm due to high CO_2 release to the atmosphere in August 2006 and July–October 2007, whereas the maximum monthly pCO_2 increase was 14–23 μatm due to CO_2 uptake by the ocean from November 2006 to February 2007.

We also find that the primary pCO_2 controlling processes varied with time of year (Fig. 7). Cooling during September–November 2006, January 2007, and October 2007, and warming in March 2007, May 2007, and June 2007 were the most important processes (temperature). Biological respiration (producing CO_2) during peak summer (July–August of 2006 and 2007), as well as in September 2007, and biological production (consuming CO_2) in April 2007 were the most important processes (biology). Mixing was the most important in February 2007 at the peak winter time when river discharge was moderately high but biological production was low and temperature was low but stable, and air–sea exchange (uptake) was the most important in December 2006. In fact, several processes often combined to influence pCO_2. For example, in September 2006 while cooling was the most important process, this effect was almost completely offset by biological respiration (Fig. 7).

Overall our work pointed out the importance of mixing (primarily horizontal transports) on surface water pCO_2, especially in river-influenced coastal oceans and our method made improvements in quantifying the contribution of mixing. Considering that the waters at the buoy site were influenced by rivers (Menzel, 1993), which transport terrestial carbon and CO_2 produced by the salt-marshes and within the estuaries to the shelf (Jiang et al., 2008b, 2013; Wang and Cai, 2004), we used monthly varying slope values of DIC–*S*, which are associated with river discharge (Fig. 3b), to estimate the contribution from horizontal transports. This estimate captured the signal of pCO_2 variability due to horizontal transports and better separated the biological signal produced in the estuarine and nearshore zone that was brought to the buoy site. In contrast, in recent studies this contribution from horizontal transports was often not separated from other controlling processes (e.g. Schiettecatte et al., 2006; Vandemark et al., 2011; Shadwick et al., 2015) or was simply quantified on the basis of a constant linear relationship of DIC and salinity observed during cruises (e.g. Shadwick et al., 2011). The method we used to separate the contributions of various processes to pCO_2 variation should be useful in exploring the mechanisms that drive coastal ocean CO_2 variations.

4.2.2. Uncertainty assessment of the 1-D model

Here we estimated the uncertainty associated with key terms in the model (Table 2). First, the uncertainty of DIC calculated from the pCO_2 and salinity-derived TA was estimated to be ~13 μmol kg^{-1} or <1% via the program CO2SYS (Lewis and Wallace, 1998) (without considering the uncertainty induced by carbonate acid dissociation constants during calculations), given the uncertainty of ~13 μmol kg^{-1} for salinity-derived TA (Fig. 3a) and the uncertainty of 2 μatm for pCO_2 measurement (Sutton et al., 2014b). The DIC uncertainty will lead to an uncertainty of 18.4 μmol kg^{-1}, or $(13^2 + 13^2)^{0.5}$, for monthly DIC changes ($\Delta DIC = DIC_2 - DIC_1$). This uncertainty, which will propagate into ΔDIC_{bio} and NCP, was very large considering that ΔDIC was often very small (Table 2), though the uncertainty associated with DIC

was minor (<1%). Second, to separate mixing and biological effects, the slope values of DIC–Salinity between the composite nearshore and open-ocean end-members during 2006–2007 was estimated from the relationship between slope values and monthly mean discharge of Altamaha River during 2005–2006 (Fig. 3b). The uncertainty associated with slope values estimated from the residual values of predicted slope values was 3% during November–May and 23% during June–October; similar uncertainties will propagate into ΔDIC_{mix}. The positive relationship during the relatively cold and wet months of November–May is strong with a ±3% uncertainty and could be due to a dilution of nearshore DIC by high discharges (thus DIC–*S* slope is greater as the nearshore DIC decreases). The negative relationship during the warm and dry months of June–October is somewhat weak with a large relative uncertainty (±23%). While it is not entirely clear what drives the negative correlation during June–October, overall a high nearshore DIC and thus a low DIC–*S* slope is expected during the period of low discharge and high marsh export and estuarine respiration. Third, the uncertainty in air–sea CO_2 exchange (up to 20%), resulting from quantifying gas transfer velocity (Wanninkhof et al., 2009; Watson et al., 2009) and the uncertainty associated with mixed layer depth (up to 15%, e.g. Shadwick et al., 2015) will act together to induce an uncertainty of ~25% for ΔDIC_{a-s}.

The uncertainties associated with ΔDIC_{bio} and NCP are estimated by propagating the uncertainty in each term on the right hand of Eqs. (8a) and (8d) ($\sqrt{\sum (\text{uncertainty})^2}$, Table 2). We find that the uncertainties associated with ΔDIC_{mix} (<2.4 μmol kg^{-1}) and ΔDIC_{a-s} (<4.8 μmol kg^{-1}) are relatively small, and in contrast there are large uncertainties associated with ΔDIC_{bio} (>18.4 μmol kg^{-1}) and NCP (>5.0 mmol m^{-2} d^{-1}) (Table 2), originating from the large uncertainty in ΔDIC. Therefore, the primary source of uncertainty can be traced back to the TA estimated from salinity. Apart from the complexity of coastal ocean (e.g. terrestrial inputs), the uncertainty in estimated TA was also associated with the seasonality of the TA–*S* relationship, which, if there is any (we assume none in this work), will cause greater uncertainty for low-salinity data and lower uncertainty for high-salinity data (Fig. s6). For the lowest salinity of 31.73 observed during 2005–2006, the difference of predicated TA by different linear fits will be up to 57 μmol kg^{-1} (Fig. s6). Fortunately, the salinity at the buoy site was generally high with an annual average of 35.47. For a salinity of 35.47, the difference of predicated TA by different linear fits will be 12 μmol kg^{-1}. Thus, more efforts in terms of improving TA estimates should be attempted to reduce the model uncertainty in future. Of course, all the uncertainties mentioned above will also propagate into pCO_2 (not shown). However, we have to point out that the uncertainty associated with ΔpCO_{2bio}, the closing term, will be smaller than ΔDIC_{bio} due to the relatively small uncertainty in pCO_2 measurement and in estimates of ΔDIC_{mix} and ΔDIC_{a-s}, even though the non-linear effect of pCO_2 was considered. The uncertainty associated with the non-linear effect (calculated from Eq. (4a)) was relatively small (1–13%) and was negligible in comparison with other uncertainties described here (ΔpCO_{2non}, the open columns in Fig. 7).

Besides the uncertainties mentioned above that have been quantified, uncertainties may also be induced by some processes that do not exist all the time or are not important at this site, and that thus are not considered in the model. For example, the effect from vertical entrainment during mixed layer deepening periods (in September) was ignored and may disturb the biological signal (the closing term). If it is assumed that the water column state in both August of 2006 and 2007 was the same as that in July 2005 (available data) and that the shift from a stratified water column to vertically well mixed waters was finished in September, an increase of 36 μmol kg^{-1} in DIC, 34 μmol kg^{-1} in TA, and 16 μatm in pCO_2 will be induced by vertical entrainment based on the method used by Shadwick et al. (2011). However, a slight increase of 0.04 in salinity during September 2006 and a great decrease of 0.79 in salinity during September 2007 (Table 2) indicate that this assumption may not be correct or that the vertical entrainment signal was masked by other process such as horizontal mixing. Since the buoy sits on a broad shallow shelf, the impact of such vertical mixing was likely very small. Using field survey data from 2005 as an example, while a slight stratification develops, DIC values in surface and bottom waters at and near the buoy site are all located on the same DIC–salinity line (Fig. s1). Therefore, in this case, vertical mixing would not introduce a signal different from horizontal mixing. However, waters below 200 m depths are clearly enriched in DIC. Occasional strong onshore advection of deep water during the summer time (which would result in lower SST and higher SSS at the buoy site, but were not observed in our data during this period; Lee et al., 1991; Menzel, 1993) thus could affect the buoy pCO_2 data in a way that is not considered in our current simple 1-D model. Finally, as noted earlier, extreme precipitation events could potentially impact our interpretation of mixing scenario and should be included in future model efforts.

4.3. Influence of enhanced river input on interannual changes in surface pCO_2

Since SSS can be a proxy for river influence at the buoy site (Fig. s5), lower SSS in September–October 2007 compared with September–October 2006 (Fig. 4b and Table 1) indicated enhanced river input to the buoy site occurring in fall 2007. Considering that rivers transport waters with excess CO_2 and organic matter from the marshes and within the estuaries to the shelf (Jiang et al., 2008b, 2013; Wang and Cai, 2004), increased surface pCO_2 in September–October 2007 was thus expected. This was confirmed by higher sea surface pCO_2 in September–October 2007 than in the comparable period of 2006 (Fig. 4 and Table 1).

Changes in river inputs resulted in different processes that control pCO_2 between September–October of 2006 and the same period of 2007 (Fig. 7). Specifically, cooling was the most important process in September 2006, and in contrast biological respiration became the most important in September 2007. Although cooling was the most important process in both October 2006 and 2007, the contribution from cooling to pCO_2 decrease was much smaller in October 2007 than in October 2006, and on the contrary, contribution to pCO_2 increase from biological respiration was greater in October 2007 than in October 2006. Although the mixing effect was not the most important process between September–October 2006 and 2007, the pCO_2 increase due to river inputs characterized by SSS was clearly enhanced in September–October 2007 compared with that in September–October 2006. Simultaneously, there were differences in monthly average NCP in September–October of 2006 and 2007 (Table 2). This site was more heterotrophic in September–October 2007 than in September–October 2006. For instance, NCP shifted from a positive value of 1.7 mmol m^{-2} d^{-1} in October 2006 to a negative value of −9.1 mmol m^{-2} d^{-1} in October 2007. Thus, in addition to direct lateral transport of high CO_2 water from salt-marshes and estuaries, higher pCO_2 in September–October 2007 was to a large extent (or even dominantly) due to greater contributions from local biological decomposition of organic matter possibly transported from the marshes and estuary (Jiang et al., 2008b, 2013; Wang and Cai, 2004).

Overall, on a river-influenced shelf, river input may cause large and less predictable variability in surface water pCO_2 and thus in air–sea CO_2 flux, highlighting the necessity of good temporal coverage for accurate estimates of air–sea CO_2 fluxes. This variability can be caused by variability in the transport of estuarine CO_2 via remote respiration occurring in the estuarine zone or respiration

of organic carbon transported from the estuarine zone. The comparison of pCO_2 in September–October 2006 and 2007 indicated that there will be large interannual variability in CO_2 at the buoy site, which can be due to varying river loading. If precipitation or wind patterns were altered by climate change and variability, the CO_2 system and CO_2 sink/source status to the atmosphere at the buoy site would also be affected by changes in these terrestrial inputs (e.g. Gypens et al., 2011).

4.4. Uncertainties in estimating air–sea CO_2 exchange and annual NCP due to under-sampling

Due to high temporal variability in CO_2 flux in this river-influenced coastal ocean (e.g. Leinweber et al., 2009; Vandemark et al., 2011; Fig. 5), we are compelled to discuss uncertainties in estimates of air–sea CO_2 fluxes and NCP due to under-sampling. We find that even a contradictory result could be obtained when ship-based surveys were conducted during seasonal transition periods or periods with episodic biological production events. During these periods sea surface pCO_2 varied rapidly between being oversaturated and undersaturated (Fig. 5). Conclusions regarding whether the study site was a CO_2 sink or source would depend on the investigation time. For instance, during early October 2006 it was a CO_2 source and later a sink (Fig. 5). During April–June 2007, it was a CO_2 sink during short periods of biological production, and otherwise it became a source (Fig. 5). This could explain why during early studies the SAB was thought to be a CO_2 source to the atmosphere (Cai et al., 2003; Wang et al., 2005), and later the entire SAB shelf was found to be a net CO_2 sink with respect to the atmosphere on an annual basis (Jiang et al., 2008a). A similar phenomenon was also found in the Southern Bight of the North Sea by Schiettecatte et al. (2007), who stated that whether or not the bloom peak in April 2002 could be captured directly determined the CO_2 sink/source status of this region on an annual basis. Under-sampling also exerted an important influence on estimates of NCP. In our case, if the short biological production events during April–May 2007 were not captured, the buoy site would become net heterotrophic even though it was still a CO_2 sink (but a smaller one). The annual NCP would be negative (from -1.04 to -0.49 mol m^{-2} yr^{-1}), if the bloom in April 2007 were not observed, and instead we used average NCP from March and May 2007 of -4.2 mmol m^{-2} d^{-1} as the NCP value in April 2007.

In all, high sampling frequency is needed in a coastal system that is susceptible to terrestrial inputs, particularly during seasonal transition periods or biological production periods for ship-based investigations. However, although the flux estimated at the buoy site should be more reliable than previous infrequent cruise-based flux estimations, it is spatially limited. A combination of high temporal resolution sampling with infrequent but whole-shelf survey cruises and synoptic satellite remote sensing approaches (e.g., Lohrenz et al., 2010; Bai et al., 2015) will give us a more complete picture of the spatial and temporal variations in the CO_2 dynamics.

5. Conclusions

Three-hour resolution observations during July 2006–October 2007 indicated that surface pCO_2 at the SAB buoy site was generally undersaturated with respect to the atmosphere in cold months (November–March) and oversaturated in warm months (April–October). These buoy observations were generally consistent with the seasonal pattern reported by previous shipboard studies (Jiang et al., 2008a). The high temporal resolution observations also revealed important events not reported in previous ship-based observations, such as the sporadically occurring biological production-induced pCO_2 drawdown during April–June 2007. Although temperature played a dominant role in an annual cycle of pCO_2, river inputs especially in the wet season, biological respiration in peak summer, and biological production during April–June 2007 also had important influences on pCO_2. The 1-D model was able to quantify the contributions of pCO_2 controlling processes and had significant implications in understanding the mechanisms driving coastal ocean CO_2 variability, and in favoring modeling work, although uncertainties existed in the model and further improvements were needed.

In addition, higher pCO_2 during September–October 2007 than during the same period a year earlier was primarily caused by increased river inputs in fall 2007. It indicated that river-influenced coastal CO_2 system was susceptible to terrestrial inputs and will exhibit large temporal variability. Thus, future research in similar coastal systems should seek to further constrain the influences on the CO_2 system and the CO_2 sink/source status from terrestrial inputs, which are modulated by human activity or climate change and variability. During the study period, on an annual basis this study site was a net CO_2 sink with respect to the atmosphere and was moderately autotrophic as shown by NCP in the mixed layer when the bloom in April–May 2007 was included during calculation. We find that temporal under-sampling could greatly bias the estimate of air–sea CO_2 fluxes or annual NCP, and even produce contradictory results, indicating the necessity of good temporal coverage in complex coastal systems.

Acknowledgements

The study was supported by the NOAA Global Carbon Cycle Program, proposal GC05-208, Ocean Acidification Program, project OAPFY11.01.NGI.003, and NSF OCE-0425153. PMEL funding was provided by the NOAA Climate Program Office and the NOAA Ocean Acidification Program. This is PMEL contribution #4260 and JISAO contribution #2399. LX thanks the China Scholarship Council for providing the scholarship fund (No. 201404180014) and National Natural Science Foundation of China (No. 41506099). We acknowledge NDBC for servicing the mooring platform. We thank Rik Wanninkhof for leading NOAA's efforts in carbon cycle research and ocean acidification monitoring in the US Gulf and East Coasts and for helpful comments on an earlier version of this paper. Finally, we acknowledge our late friend and colleague Y. Wang, who had installed and serviced the sensors on the Gray's Reef NDBC buoy during the period that data were collected and presented here.

Appendix A. Supplementary material

Supplementary data associated with this article can be found, in the online version, at http://dx.doi.org/10.1016/j.pocean.2015.09.008.

References

Atkinson, L.P., Blanton, J.O., Chandler, W.S., Lee, T.N., 1983. Climatology of the southeastern United States continental shelf waters. Journal of Geophysical Research 88, 4705–4718.

Bai, Y., Cai, W.-J., He, X., Zhai, W., Pan, D., Dai, M., Yu, P., 2015. A mechanistic semi-analytical method for remotely sensing sea surface pCO_2 in river-dominated coastal oceans: a case study from the East China Sea. Journal of Geophysical Research: Oceans. http://dx.doi.org/10.1002/2014JC010632.

Bates, N., Astor, Y., Church, M., Currie, K., Dore, J., Gonaález-Dávila, M., Lorenzoni, L., Muller-Karger, F., Olafsson, J., Santa-Casiano, M., 2014. A time-series view of changing ocean chemistry due to ocean uptake of anthropogenic CO_2 and ocean acidification. Oceanography 27, 126–141.

Bauer, J.E., Cai, W.-J., Raymond, P.A., Bianchi, T.S., Hopkinson, C.S., Regnier, P.A., 2013. The changing carbon cycle of the coastal ocean. Nature 504, 61–70.

Benway, H.M., Doney, S.C., 2014. Scientific outcomes and future challenges of the ocean carbon and biogeochemistry program. Oceanography 27 (1), 106–107. http://dx.doi.org/10.5670/oceanog.2014.13.

Boehme, S.E., Sabine, C.L., Reimers, C.E., 1998. CO_2 fluxes from a coastal transect: a time-series approach. Marine Chemistry 63, 49–67.
Borges, A.V., Delille, B., Frankignoulle, M., 2005. Budgeting sinks and sources of CO_2 in the coastal ocean: diversity of ecosystems counts. Geophysical Research Letters 32, L14601. http://dx.doi.org/10.1029/2005GL023053.
Cai, W.-J., 2011. Coastal ocean carbon paradox: CO_2 sinks or sites of terrestrial carbon incineration. Annual Review of Marine Science 3, 123–145.
Cai, W.-J., Hu, X., Huang, W., Jiang, L.-Q., Wang, Y., Peng, T., Zhang, X., 2010. Alkalinity distribution in the western North Atlantic Ocean margins. Journal of Geophysical Research: Oceans 115, C08014. http://dx.doi.org/10.1029/2009JC005482.
Cai, W.-J., Wang, Y., Hodson, R.E., 1998. Acid–base properties of dissolved organic matter in the estuarine waters of Georgia, USA. Geochimica et Cosmochimica Acta 62, 473–483.
Cai, W.-J., Pomeroy, L.R., Moran, M.A., Wang, Y., 1999. Oxygen and carbon dioxide mass balance for the estuarine–intertidal marsh complex of five rivers in the southeastern U.S. Limnology and Oceanography 44, 639–649.
Cai, W.-J., Wang, Y., 1998. The chemistry, fluxes, and sources of carbon dioxide in the estuarine waters of the Satilla and Altamaha Rivers, Georgia. Limnology and Oceanography 43, 657–668.
Cai, W.-J., Wang, Z.A., Wang, Y., 2003. The role of marsh-dominated heterotrophic continental margins in transport of CO_2 between the atmosphere, the land–sea interface and the ocean. Geophysical Research Letters 30 (16), 1849. http://dx.doi.org/10.1029/2003GL017633.
Chen, C.T.A., Huang, T.H., Chen, Y.C., Bai, Y., He, X., Kang, Y., 2013. Air–sea exchanges of CO_2 in the world's coastal seas. Biogeosciences 10, 6509–6544.
Chierici, M., Fransson, A., Nojiri, Y., 2006. Biogeochemical processes as drivers of surface fCO_2 in contrasting provinces in the subarctic North Pacific Ocean. Global Biogeochemical Cycles 20, GB1009. http://dx.doi.org/10.1029/2004GB002356.
Dickson, A.G., Millero, F.J., 1987. A comparison of the equilibrium constants for the dissociation of carbonic acid in seawater media. Deep Sea Research Part A 34, 1733–1743.
Ducklow, H.W., Doney, S.C., Steinberg, D.K., 2009. Contributions of long-term research and time-series observations to marine ecology and biogeochemistry. Annual Review of Marine Science 1, 279–302.
Fennel, K., Wilkin, J., 2009. Quantifying biological carbon export for the northwest North Atlantic continental shelves. Geophysical Research Letters 36, L18605. http://dx.doi.org/10.1029/2009GL039818.
Friis, K., Körtzinger, A., Wallace, D.W.R., 2003. The salinity normalization of marine inorganic carbon chemistry data. Geophysical Research Letters 30 (2), 1085. http://dx.doi.org/10.1029/2002GL015898.
Garcia, H.E., Gordon, L.I., 1992. Oxygen solubility in seawater: better fitting equations. Limnology and Oceanography 37, 1307–1312.
Gattuso, J.P., Frankignoulle, M., Wollast, R., 1998. Carbon and carbonate metabolism in coastal aquatic ecosystems. Annual Review of Ecology and Systematics Annual Review of Ecology and Systematics 29, 405–434.
Gruber, N., 2014. Ocean biogeochemistry: carbon at the coastal interface. Nature: News & Views. http://dx.doi.org/10.1038/nature14082.
Gypens, N., Lacroix, G., Lancelot, C., Borges, A.V., 2011. Seasonal and inter-annual variability of air–sea CO_2 fluxes and seawater carbonate chemistry in the Southern North Sea. Progress in Oceanography 88, 59–77.
Ho, D.T., Law, C.S., Smith, M.J., Schlosser, P., Harvey, M., Hill, P., 2006. Measurements of air–sea gas exchange at high wind speeds in the Southern Ocean: implications for global parameterizations. Geophysical Research Letters 33, L16611. http://dx.doi.org/10.1029/2006GL026817.
Jiang, L.-Q., Cai, W.-J., Wanninkhof, R., Wang, Y., Lüger, H., 2008a. Air–sea CO_2 fluxes on the U.S. South Atlantic Bight: spatial and seasonal variability. Journal of Geophysical Research: Oceans 113, C07019. http://dx.doi.org/10.1029/2007JC004366.
Jiang, L.-Q., Cai, W.-J., Wang, Y., 2008b. A comparative study of carbon dioxide degassing in river- and marine-dominated estuaries. Limnology and Oceanography 53, 2603–2615.
Jiang, L.-Q., Cai, W.-J., Wang, Y., Bauer, J.E., 2013. Influence of terrestrial inputs on continental shelf carbon dioxide. Biogeosciences 10, 839–849.
Körtzinger, A., Send, U., Wallace, D.W.R., Karstensen, J., DeGrandpre, M., 2008. Seasonal cycle of O_2 and pCO_2 in the central Labrador Sea: atmospheric, biological, and physical implications. Global Biogeochemical Cycles 22, GB1014. http://dx.doi.org/10.1029/2007GB003029.
Laruelle, G.G., Lauerwald, R., Pfeil, B., Regnier, P., 2014. Regionalized global budget of the CO_2 exchange at the air–water interface in continental shelf seas. Global Biogeochemical Cycles 28. http://dx.doi.org/10.1002/2014GB004832.
Lee, T.N., Yoder, J.A., Atkinson, L.P., 1991. Gulf Stream frontal eddy influence on productivity of the southeast U.S. Continental Shelf. Journal of Geophysical Research: Oceans 96, 22191–22205.
Leinweber, A., Gruber, N., Frenzel, H., Friederich, G.E., Chavez, F.P., 2009. Diurnal carbon cycling in the surface ocean and lower atmosphere of Santa Monica Bay, California. Geophysical Research Letters 36, L08601. http://dx.doi.org/10.1029/2008GL037018.
Lewis, E., Wallace, D.W.R., 1998. Program developed for CO_2 systems calculations. ORNL/CDIAC 105. Carbon Dioxide Information Analysis Center, Oak Ridge National Laboratory US Department of Energy, Oak Ridge, Tennessee.
Lohrenz, S.E., Cai, W.-J., Chen, F., Chen, X., Tuel, M., 2010. Seasonal variability in air–sea fluxes of CO_2 in a river-influenced coastal margin. Journal of Geophysical Research: Oceans 115, C10034. http://dx.doi.org/10.1029/2009JC005608.
Mehrbach, C., Culberson, C.H., Hawley, J.E., Pytkowicz, R.M., 1973. Measurement of the apparent dissociation constants of carbonic acid in seawater at atmospheric pressure. Limnology and Oceanography 18, 897–907.
Menzel, D.W., 1993. Ocean Processes: U.S. Southeast Continental Shelf: A Summary of Research Conducted in the South Atlantic Bight under the Auspices of the U.S. Department of Energy from 1977–1991. U.S. DOE.
Muller-Karger, F.E., Varela, R., Thunell, R., Luerssen, R., Hu, C., Walsh, J.J., 2005. The importance of continental margins in the global carbon cycle. Geophysical Research Letters 32, L01602. http://dx.doi.org/10.1029/2004GL021346.
Redfield, A.C., Ketchum, B.H., Richards, F.A., 1963. The influence of organisms on the composition of sea water. In: Hill, M.N. (Ed.), The Sea. Interscience, New York, pp. 26–77.
Schiettecatte, L., Gazeau, F., van der Zee, C., Brion, N., Borges, A.V., 2006. Time series of the partial pressure of carbon dioxide (2001–2004) and preliminary inorganic carbon budget in the Scheldt plume (Belgian coastal waters). Geochemistry, Geophysics, Geosystems 7 (6), Q06009. http://dx.doi.org/10.1029/2005GC001161.
Schiettecatte, L.S., Thomas, H., Bozec, Y., Borges, A.V., 2007. High temporal coverage of carbon dioxide measurements in the Southern Bight of the North Sea. Marine Chemistry Special issue: Dedicated to the memory of Professor Roland Wollast 106, 161–173.
Shadwick, E.H., Thomas, H., Azetsu-Scott, K., Greenan, B.J.W., Head, E., Horne, E., 2011. Seasonal variability of dissolved inorganic carbon and surface water pCO_2 in the Scotian Shelf region of the Northwestern Atlantic. Marine Chemistry 124 (1–4), 23–37.
Shadwick, E.H., Trull, T.W., Tilbrook, B., Sutton, A.J., Schulz, E., Sabine, C.L., 2015. Seasonality of biological and physical controls on surface ocean CO_2 from hourly observations at the Southern Ocean Time Series site south of Australia. Global Biogeochemical Cycles 29, 223–238. http://dx.doi.org/10.1002/2014GB004906.
Signorini, S.R., Mannino, A., Najjar, R.G., Friedrichs, M.A.M., Cai, W.-J., Salisbury, J., Wang, Z.A., Thomas, H., Shadwick, E., 2013. Surface ocean pCO_2 seasonality and sea–air CO_2 flux estimates for the North American east coast. Journal of Geophysical Research: Oceans 118, 1–22. http://dx.doi.org/10.1002/jgrc.20369.
Sutton, A.J., Feely, R.A., Sabine, C.L., McPhaden, M.J., Takahashi, T., Chavez, F.P., Friederich, G.E., Mathis, J.T., 2014a. Natural variability and anthropogenic change in equatorial Pacific surface ocean pCO_2 and pH. Global Biogeochemical Cycles 28, 131–145. http://dx.doi.org/10.1002/2013GB004679.
Sutton, A.J., Sabine, C.L., Maenner-Jones, S., Lawrence-Slavas, N., Meinig, C., Feely, R.A., Mathis, J.T., Musielewicz, S., Bott, R., McLain, P.D., Fought, H.J., Kozyr, A., 2014b. A high-frequency atmospheric and seawater pCO_2 data set from 14 open-ocean sites using a moored autonomous system. Earth System Science Data 6, 353–366.
Sweeney, C., Gloor, E., Jacobson, A.R., Key, R.M., McKinley, G., Sarmiento, J.L., Wanninkhof, R., 2007. Constraining global air–sea gas exchange for CO_2 with recent bomb 14C measurements. Global Biogeochemical Cycles 21, GB2015. http://dx.doi.org/10.1029/2006GB002784.
Takahashi, T., Olafsson, J., Goddard, J.G., Chipman, D.W., Sutherland, S.C., 1993. Seasonal variation of CO_2 and nutrients in the high-latitude surface oceans: a comparative study. Global Biogeochemical Cycles 7, 843–878.
Vandemark, D., Salisbury, J.E., Hunt, C.W., Shellito, S.M., Irish, J.D., McGillis, W.R., Sabine, C.L., Maenner, S.M., 2011. Temporal and spatial dynamics of CO_2 air–sea flux in the Gulf of Maine. Journal of Geophysical Research: Oceans 116, C01012. http://dx.doi.org/10.1029/2010JC006408.
Wang, Z.A., Cai, W.-J., Wang, Y., Ji, H., 2005. The southeastern continental shelf of the United States as an atmospheric CO_2 source and an exporter of inorganic carbon to the ocean. Continental Shelf Research 25, 1917–1941.
Wang, Z.A., Cai, W.-J., 2004. Carbon dioxide degassing and inorganic carbon export from a marsh-dominated estuary (the Duplin River): a marsh CO_2 pump. Limnology and Oceanography 49, 341–354.
Wanninkhof, R., 1992. Relationship between wind speed and gas exchange over the ocean. Journal of Geophysical Research 97, 7373–7382.
Wanninkhof, R., Asher, W.E., Ho, D.T., Sweeney, C., McGillis, W.R., 2009. Advances on quantifying air–sea gas exchange and environmental forcing. Annual Review of Marine Science 1, 213–244.
Watson, A.J., Schuster, U., Bakker, D.C.E., Bates, N.R., Corbière, A., González-Dávila, M., Friedrich, T., Hauck, J., Heinze, C., Johannessen, T., Körtzinger, A., Metzl, N., Olafsson, J., Olsen, A., Oschlies, A., Padin, X.A., Pfeil, B., Santana-Casiano, J.M., Steinhoff, T., Telszewski, M., Rios, A.F., Wallace, D.W.R., Wanninkhof, R., 2009. Tracking the variable North Atlantic sink for atmospheric CO_2. Science 326, 1391–1393.
Weiss, R.F., 1974. Carbon dioxide in water and seawater: the solubility of a non-ideal gas. Marine Chemistry 2, 203–215.
Weiss, R.F., Price, B.A., 1980. Nitrous oxide solubility in water and seawater. Marine Chemistry 8, 347–359.
Willcox, S., Meinig, C., Sabine, C.L., Lawrence-Slavas, N., Richardson, T., Hine, R., Manley, J., 2010. An autonomous mobile platform for underway surface carbon measurements in open-ocean and coastal waters OCEANS 2009. MTS/IEEE Biloxi-Marine Technology for Our Future: Global and Local Challenges. IEEE, pp. 1–8.
Xue, L., Xue, M., Zhang, L., Sun, T., Guo, Z., Wang, J., 2012. Surface partial pressure of CO_2 and air–sea exchange in the northern Yellow Sea. Journal of Marine Systems 105–108, 194–206.